Published in final edited form as:
Metab Brain Dis. 2014 June ; 29(2): 323–332. doi:10.1007/s11011-014-9487-6.

A comparison of spectral quality in magnetic resonance spectroscopy data acquired with and without a novel EPI-navigated PRESS sequence in school-aged children with fetal alcohol spectrum disorders

Aaron T. Hess, Ph.D.[1,2,3], **Sandra W. Jacobson, Ph.D.**[2,4,5], **Joseph L. Jacobson, Ph.D.**[2,4,5], **Christopher D. Molteno, M.D.**[5], **André J.W. van der Kouwe, Ph.D.**[6], and **Ernesta M. Meintjes, Ph.D.**[1,2]

[1]MRC/UCT Medical Imaging Research Unit, Faculty of Health Sciences, University of Cape Town, Cape Town, South Africa

[2]Department of Human Biology, Faculty of Health Sciences, University of Cape Town, Cape Town, South Africa

[3]University of Oxford Centre for Clinical Magnetic Resonance Research, Oxford, UK

[4]Department of Psychiatry and Behavioral Neurosciences, Wayne State University School of Medicine, Detroit, Michigan, USA

[5]Department of Psychiatry and Mental Health, Faculty of Health Sciences, University of Cape Town, Cape Town, South Africa

[6]Department of Radiology and Athinoula A. Martinos Center for Biomedical Imaging, Massachusetts General Hospital, Boston, Massachusetts, USA

Abstract

Single voxel spectroscopy (SVS) can generate useful information regarding metabolite concentrations provided that the MR signal can be averaged over several minutes during which the subject remains stationary. This requirement can be particularly challenging for children who cannot otherwise be scanned without sedation. To address this problem we developed an EPI volume navigated (vNav) SVS PRESS sequence, which applies real-time head pose (location and orientation), frequency, and first-order B0 shim adjustments. A water-independent preprocessing algorithm removes residual frequency and phase shifts resulting from within-TR movements. We compare results and performance of the standard and vNav PRESS sequences in a sample of 9- to 10-year-olds from a South African cohort of children with fetal alcohol spectrum disorders (FASD) and healthy controls. Magnetic resonance spectroscopy (MRS) data in the deep cerebellar nuclei were initially acquired with the standard PRESS sequence. The children were re-scanned 1 year later with the vNav PRESS sequence. Good quality data were acquired in 73% using the

Corresponding author(s): Ernesta M. Meintjes, Ph.D., Department of Human Biology, Faculty of Health Sciences, University of Cape Town, Observatory, 7925, South Africa, Tel. +27 21-406-6547, Fax +27 21-448-7226, ernesta.meintjes@gmail.com. Sandra W. Jacobson, Ph.D., Department of Psychiatry and Behavioral Neurosciences, Wayne State University School of Medicine, 3901 Chrysler Drive, Suite 2-C, Detroit, MI 48201, USA, Tel. +1-313-993-5454, Fax +1-313-993-3427 fax, sandra.jacobson@wayne.edu.

The authors declare no competing financial interests.

vNav PRESS sequence, compared to only 50% for the standard PRESS sequence. Additionally, tighter linewidths and smaller variances in the measured concentrations were observed. These findings confirm previous reports demonstrating the efficacy of our innovative vNav sequence with healthy volunteers and young children with HIV and expand its application to a school-aged population with FASD—disorders often associated with attention problems and hyperactivity. This study provides the most direct evidence to date regarding degree to which these new methods can improve data quality in research studies employing MRS.

Keywords

magnetic resonance spectroscopy; motion correction; B0 correction; EPI navigator; fetal alcohol spectrum disorders; South Africa

Introduction

Single voxel spectroscopy (SVS) can provide useful information regarding metabolite concentrations when the spectra are acquired within the intended anatomy with a constant frequency and optimal main magnetic field (B0). Acquiring these spectra is usually straightforward, provided subjects remain stationary during the scanning session and scan adjustments are appropriately performed. However, when movement occurs, it can go undetected and lead to acquisition of spectra from the wrong anatomical regions and spectral artifacts, such as frequency shifts and line shape distortions. Several minutes of signal averaging may be necessary, which is often not possible for restless or uncomfortable children, particularly those with developmental brain disorders, such as attention deficit hyperactivity disorder (ADHD) or fetal alcohol spectrum disorders (FASD), among whom attention problems and hyperactivity are common (e.g., Coles et al. 1997; J. Jacobson et al. 2011; Mattson et al. 2011). We have previously demonstrated the benefits of using an echo planar imaging (EPI) volume navigated (vNav) Point Resolved Spectroscopy (PRESS) sequence with normal adult volunteer subjects (Hess et al. 2011; 2012) and with a sample of young HIV-exposed children (Hess et al. in press). In this study we extend these findings by demonstrating the benefits of using an EPI vNav PRESS sequence in a sample of 9- to 10-year-old school-aged Cape Coloured (mixed ancestry) children who are participating in a prospective longitudinal study on FASD in Cape Town, South Africa (Jacobson et al. 2008).

The vNav is capable of measuring within each TR head pose (location and orientation), zero-order B0 offset (implemented as RF transmit/receive frequency), and spatially higher-order B0 offsets (implemented with shim gradients of which the linear terms are adjustable in real time). We present a comparison of the results obtained with the standard and vNav PRESS sequences. In this comparison the spectra were obtained in a cerebellar volume of interest (VOI).

Head pose tracking is important in SVS as there is no way of confirming whether all measurements were acquired from the same volume. In this respect, spectroscopy differs from imaging, where blurring and artifacts are apparent in the resulting image in the presence of motion. In SVS, which uses large voxels, such as $20 \times 20 \times 20$ mm^3, voxel shifts on the order of 2 to 3 mm may seem inconsequential. However, if the movement is

enough to alter the gray/white matter ratio, mechanisms for partial volume correction will be rendered invalid. By using the vNav to perform head pose correction, one can ensure that the measurements are consistently acquired from the same anatomical region.

FASD is characterized by a broad range of irreversible neuropsychological deficits, including poorer IQ—Full Scale IQ in children with FAS (Streissguth et al. 1990; Mattson et al. 1997; Jacobson et al. 2008, 2011) and problems in the Freedom from Distractibility domain comprised of Arithmetic and Digit Span in more moderately exposed children (Jacobson et al., 2004). Eyeblink conditioning is also exceptionally sensitive to prenatal alcohol exposure (Jacobson et al. 2008, 2011). Eyeblink conditioning, which has also been linked to effects of alcohol exposure in animals, is a cerebellar-mediated nonverbal classical conditioning paradigm, in which the subject learns to associate a conditioned stimulus, typically a pure tone, with a brief air puff to the eye (unconditioned stimulus) that elicits a reflexive blink. In the 5-year follow-up of our Cape Town Longitudinal Cohort, none of the children with full fetal alcohol syndrome (FAS) met criteria for conditioning, compared to 75% of the healthy controls; only 33.3% of the children with partial FAS (PFAS) and 37.9% of the heavily exposed nonsyndromal children met criteria for conditioning (Jacobson et al., 2008). These findings were subsequently confirmed in a school-aged cohort (Jacobson et al., 2011). FAS, the most severe form of FASD, is characterized by distinctive craniofacial dysmorphology (short palpebral fissures, thin upper lip, flat or smooth philtrum), small head circumference, and growth retardation (Stratton et al. 1996). PFAS is diagnosed when there is a history of heavy maternal drinking during pregnancy, the presence of two or more of the principal alcohol-related facial anomalies, and small head circumference, growth retardation, or cognitive and/ or behavioral dysfunction (Hoyme et al., 2005).

The most recent studies of the incidence of FAS and PFAS combined in the Cape Coloured population in the Northern and Western Cape Provinces of South Africa has been estimated to be 88–89 per 1000, which is among the highest in the world (May et al. 2007; May and Gossage 2011; Urban et al. 2008). This population, composed mainly of descendants of white European settlers, Malaysian slaves, Khoi-San aboriginals, and black Africans, has historically comprised the large majority of workers in the wine-producing region of the Western Cape. The high prevalence of FAS in this community is a consequence of very heavy maternal drinking during pregnancy (Croxford and Viljoen 1999), which is due to poor psychosocial circumstances and the traditional *dop* system, in which farm laborers were paid, in part, with wine. Although the *dop* system has been outlawed since the 1920s, heavy alcohol consumption persists in a high proportion (~30%) of women during pregnancy in this community (Jacobson et al. 2006; Jacobson et al. 2008) despite extensive efforts to intervene to reduce pregnancy drinking.

The high prevalence of heavy alcohol consumption during pregnancy in a single cohort is unusual and led to our conducting the first prospective study of FAS beginning in pregnancy (Carter et al. 2005; Jacobson et al. 2008; Molteno et al. in press). Within the context of this research program, we conducted the first functional MRI studies in South Africa (Cheng et al. in press; Diwadkar et al. 2013; Meintjes et al. 2010), which contributed to the establishment of the research-dedicated Cape Universities Brain Imaging Centre (CUBIC). Extensive pediatric neuroimaging research is currently being conducted by numerous

research groups at CUBIC, including development of innovative methodological techniques, such as the one examined here. In this study, magnetic resonance spectroscopy (MRS) was administered initially to a sample of 56 nonsedated children from our longitudinal FASD cohort with a standard PRESS sequence at age 9 years and again 1 year later with the novel vNav PRESS sequence, providing a unique opportunity to examine the degree to which the latter can improve spectral quality.

The aim of the present study was to compare the quality, accuracy, and measurement variance in the spectroscopy data acquired in these nonsedated school-aged children with FASD using the standard and vNav PRESS sequences.

Methods and Applications

Study Participants

The sample consisted of 59 Cape Coloured children (30 males, 29 females) born between 1999–2001 whose mothers were recruited during pregnancy to participate in a longitudinal study of FASD (Jacobson et al. 2008). Forty-three of these children were heavily exposed prenatally to alcohol; of the 16 healthy controls, 15 were born to women who abstained from drinking and 1 to a woman who drank minimally during pregnancy (i.e., 2 drinks on 3 occasions). The mothers who drank during pregnancy averaged 1.0 oz absolute alcohol or the equivalent of 2 standard drinks/day (Table 1). However, they concentrated their drinking to 1–2 days/week, thereby consuming an average of 7.1 standard drinks/occasion. In 2005 we organized an FASD diagnostic clinic in which each of the children were examined by two expert dysmorphologists: 9 (20.9%) of the heavily alcohol exposed children were diagnosed with FAS; 19 (44.2%) with PFAS); 15 (34.9%) were classified as nonsyndromal heavily exposed (HE) children. As expected, heavy drinkers smoked more than controls. Only three women reported using marijuana during pregnancy, one used cocaine, and none used methaqualone (“mandrax”). IQ was assessed on the Wechsler Intelligence Scale for Children-IV (WISC-IV; Wechsler, 2003) at 9 years (see detailed description in Jacobson et al., 2011 and Diwadkar et al., 2013). As we have previously reported (e.g., Jacobson et al., 2008, 2011), there was a dose-dependent effect of prenatal alcohol on the WISC IQ test. In 2009, when the children were 9.4 years of age (SD=0.4), data were acquired from 56 of the children in the deep cerebellar nuclei (Fig. 1) using a standard PRESS sequence. In 2010, when the children were 10.4 years (SD=0.4), MRS scan data were acquired from 52 children in the same region using the EPI volume navigated (vNav) PRESS sequence. Table 1 presents the breakdown per group for the populations scanned in 2009 and 2010.

Scan Protocol and Subject Preparation

Pre-scan preparation included practice in a mock scanner where each child was exposed to the noises and feeling of being in a tunnel, followed by a tour of the scanner. The child was then given the choice of whether to continue with scanning or not. It was made clear that s/he could terminate the scan at any time should s/he wish and that a research nurse/assistant would be present in the scan room at all times. During both scans, the child watched a video (e.g., *Finding Nemo*), using standard headphones. Heads were tightly packed in the head coil with foam pillows to minimise head motion. All scans were acquired according to protocols

that had been approved by both the Faculty of Health Sciences Human Research Ethics Committee at the University of Cape Town and the Institutional Review Board of Wayne State University. The mother or father provided written informed consent; all children provided oral assent.

All scans were acquired on a 3T Allegra (Siemens, Erlangen, Germany) MRI scanner with a birdcage transmit-receive head coil. The protocol consisted of (1) a three plane localiser, (2) a vNav set sequence (duration 1 s), which sets the navigator position, acquired only for the 2010 scans that used the vNav PRESS sequence, (3) T2 weighted acquisitions in three orientations to localise the cerebellar deep nuclei due to signal loss in this region arising from iron deposits (Dimitrova et al., 2006) (TR = 2 s, TE = 88 ms, Echo Train Length = 5, slice thickness = 3 mm, and resolution $0.9 \times 1.2 \times 3$ mm^3), and (4) the SVS acquisition using either the standard PRESS acquisition (2009) or the vNav PRESS sequence (2010). PRESS scan parameters were voxel size $20 \times 12 \times 16$ mm^3, 128 measurements, TE = 30 ms, TR = 2 s, and bandwidth = 1000 Hz. Vector sizes of 1024 and 512 were used for the standard and vNav PRESS sequences, respectively.

The vNav uses Prospective Acquisition CorrEction (PACE) (Thesen et al. 2000) to register each navigator to the navigator from the first TR (post preparation scans) in order to correct head pose. In addition, the sequence employs a dual-contrast 3D EPI sequence module to generate within each TR a B0 field map and calculate the absolute frequency and first order B0 gradient for the intended VOI. In this manner the absolute head position, frequency in the VOI, and first-order shim in the VOI are updated by the navigator each TR. Additionally, a frequency and first-order shim appropriate to the larger field of view of the navigator itself are calculated and applied to each TR.

The vNav protocol was as follows: resolution $5 \times 5 \times 5$ mm^3, FOV $220 \times 200 \times 110$ mm^3, matrix 44×40, 22 partitions, TE_1 8 ms, and TE_2 12.8 ms, TR 21 ms, flip angle 2°, bandwidth 3906 Hz/px. The orientation was set by the operator and chosen to cover the intended VOI in addition to maximally covering the brain, as shown in Figure 1. The duration of the vNav sequence module was 966 ms and the online processing, including pose, frequency, and shim calculations, took 170 ms per navigator.

Offline phase- and frequency-corrected averaging

We developed a method to perform offline frequency- and phase-corrected averaging. This method, which is independent of the residual water in each FID, consists of three steps: i) residual water peak removal, ii) frequency detection by cross-correlation with a simulated spectrum, and iii) complex combination weighting determined by singular value decomposition (SVD). All processing is performed in the spectral domain and upsampled to a frequency resolution of 0.49 Hz. Prior to any processing, a copy of the spectrum acquired in each TR without any water editing is retained for the final averaging. Water peak removal is necessary before preprocessing as it improves the cross-correlation baseline and more importantly prevents fluctuations in the water saturation from biasing the SVD. A comprehensive model spectrum was simulated using jMRUI NMR Scope (Graverondemilly et al. 1993) for the same sequence described above and a linewidth of 2 Hz. The model spectra included choline, creatine (Cr), phosphocreatine, phosphocholine, GABA,

glutamate, glutamine, myo-inositol (INS), N-acetylaspartate (NAA), and N-acetylaspartylglutamate (NAAG). The range of −3.5 ppm to −1 ppm was cross-correlated with each spectrum to detect its frequency offset and thus re-align both the original (non water-edited) and water-edited spectra appropriately.

SVD is applied in the range −3.5 ppm to −1 ppm to the water-edited and frequency-adjusted spectra. The output of the SVD operation is the set of matrices **U**, **S**, and **V,** where **U** and **V** describe the right and left singular vectors, entries on the diagonal of **S** are the singular values, and $\mathbf{USV}^T$ equals the input spectra. The first row of **V** is a complex set of weights applied to each non-water edited spectrum ($\mathbf{O_s}$), which are summed and multiplied by the mean of the first row of **V**. This process regenerates the left hand singular vectors using the original unedited spectra with appropriate scaling.

The preprocessing steps described above could only be applied to the scans that employed the vNav because scans acquired with the standard PRESS sequence did not record individual measurements prior to averaging.

Spectral Analysis

The first criterion in determining the success of a technique is how much of the data is usable. Our criteria for exclusion of data were linewidths greater than 0.08 ppm (9.9 Hz) or signal-to-noise ratio (S/N) less than 8. We also added a visual check of the spectra to ensure they conformed to the spectral plot expected (i.e., no large unknown signals or other type of interference). The excluded data were eliminated from further processing.

The vNav records the motion and shim corrections applied in a log file. These logs were used to calculate the absolute position of the SVS voxel relative to the initial reference position throughout the scan, and thus determine the extent of subject movement during the scan.

All metabolite analyses were performed in LCModel (Provencher 2001), where a water reference spectrum was used for water and eddy current correction. The measures used from LCModel were the metabolite concentrations, their percent standard deviation (%SD), linewidth, and S/N.

Results

Only 28 of the 56 scans acquired in 2009 without the vNav provided spectra of suitable quality (50% success rate); whereas in 2010, with the vNav, 39 of the 41 (95%) completed scans provided spectra of suitable quality (Fig. 2), i.e., only two of the scans did not meet our quality criteria. Spectra for 11 subjects were not acquired at the second scan due to navigator-related failures listed in Table 2, giving a 73% success rate from the total of 52 scans. Using the standard PRESS acquisition, only 33.3% of the children with FAS provided good spectra, compared with 57.1% of the controls. Using the vNav PRESS, good spectra were obtained from 71.4% and 75.0% of the children with FAS and controls, respectively, with all failures resulting from technical difficulties with the vNav. The proportion of good spectra for the PFAS children increased from 50.0% to 83.3%; for the heavily exposed

nonsyndromal, from 60.0% to 66.7%. Thus, whereas the vNav PRESS was associated with improved spectral quality within all four groups, the benefit was greatest for the most severely affected FAS group.

The reference vNav volume and associated field map for one of the scans is shown in Figure 3. To quantify the extent to which the scans were affected by motion, we have plotted box-and-whisker plots of the maximum absolute vector translations and rotations of the child's head from the start of the scan, expressed firstly about the centre of the navigator volume, representing gross head translation and rotation, and secondly about the centre of the SVS voxel, translations only. (Fig. 4). Displacements were calculated using the motion estimates of the vNav that are recorded in a log file. None of the scans exhibited more than 3 mm maximum absolute voxel displacement.

Figure 5 compares the mean and standard deviation of the linewidth and S/N using the standard and navigated PRESS sequences. There is a clear improvement in both the mean linewidth ($p = 0.03$) and S/N ($p = 0.0001$) in the 2010 scans compared to the 2009 scans.

Over and above the quality measures of linewidth and S/N, we wanted to assess the consistency of the measured metabolite concentrations. To compare the variance and range of metabolite concentrations, we have plotted box-and-whisker plots in Figure 6 of the concentrations in the nonalcohol-exposed control children for the 2009 (standard PRESS) and 2010 (vNav PRESS) scans, respectively. Data points were excluded from this plot if % SD exceeded 30%. The following metabolites are shown: NAA, INS, Cr, NAAG, and guanidoacetate (GUA).

Discussion

This study provides new evidence for the efficacy of our EPI volume navigated single voxel spectroscopy PRESS sequence for school-aged children with developmental brain disorders, such as FASD and ADHD that may make it difficult for the participant to remain stationary over the several minutes required by the MRS scan. This new PRESS sequence applies real time head pose (location and orientation), frequency, and first-order B0 shim adjustments. The present study extends our previous findings in which our novel vNav PRESS sequence was used successfully with healthy volunteers (Hess et al. 2011; 2012) and with young children with HIV (Hess et al. in press) to a pediatric population with FASD. In a direct comparison of the quality of the data generated by the standard and vNav PRESS sequences, we found a 50% increase in the number of usable scans, as well as significant improvements in linewidth and S/N. As reported above, the improvement was greatest in the most severely impaired group—children with full FAS—who had provided the fewest usable scans (only 33%) using the standard PRESS acquisition. Thus, these data provide support for the suggestion that the SVS motion correction may be especially useful in studies of difficult or developmentally disabled populations of children, who may be prone to inattention or difficulty inhibiting movement.

While prospective frequency adjustment corrects the system frequency for TR-to-TR changes, pose changes within TR may still result in both residual frequency and phase

variations. These phase variations result from the velocity encoding effect of the PRESS (or STEAM) gradients. Detecting the frequency and phase shift of each measurement enables constructive averaging. Methods that use the residual water signal within the spectra (Ernst and Li 2009; Helms and Piringer 2001; Star-Lack et al. 2000) or a high signal metabolite peak to detect the frequency and phase for each measurement (Gabr et al. 2006; Waddell et al. 2007) have been proposed. In cases where complete water suppression is employed, the frequency and phase of the residual water may be misleading due to the relative shift in the suppression band that results in asymmetric water saturation. We present a post-processing technique that is independent of the residual water and uses the spectral range from −3.5 ppm to −1 ppm for both frequency and phase correction.

In the first scan, standard PRESS without the vNav, only 50% of the spectra were usable due to poor spectral quality. As no motion tracking was performed, we can only speculate as to the reason for these failures. We suspect that the main problem was poor B0 shimming in the cerebellar VOI. In the follow-up scan performed 1 year later with the vNav, no significant motion correction was applied (motion never exceeded 3mm), and yet 73% of subjects scanned yielded good data. In contrast to the standard PRESS acquisitions, the vNav PRESS sequence provided good spectral quality in all but two scans with the remaining failures occurring as a result of technical failures with the new sequence. These technical failures would not have been present in a standard PRESS sequence. These failures are discussed below and solutions are suggested to prevent them from happening in the future. Some portion of this improvement in spectral quality may be attributable to the increased maturity of the subjects (1 year), and their past experience in the scanner may have made them less restless. However, these factors do not seem sufficient to explain an improvement of this magnitude, particularly since, as we have reported in a subsequent study, more optimal linewidths were seen in a sample of 5-year-old children with HIV when they were scanned for the first time using vNav PRESS (Hess et al. in press). We, therefore, conclude that the combination of vNav shimming with offline frequency and phase correction are primarily responsible for generating the higher quality spectra. The scans within quality bounds saw a mean linewidth reduction of 1.2 Hz and an S/N improvement of 2.5 (from 9.6 to 12.1) when using the vNav and offline preprocessing. The effect of this improvement in spectral quality is apparent with the reduced range and variance of several metabolites, as shown in Figure 6.

We encountered three causes of failures for the vNav scans. The first and most prevalent (n=5) was observed in the EPI B0 field maps of the vNav, where an error in the phase unwrapping resulted in a 208 Hz (2π) phase offset at the cerebellar voxel of interest. This type of error is typical in B0 field maps of this kind where no absolute reference frequency is present. We have since introduced a simple algorithm to avoid this problem in the future. The algorithm uses the prior knowledge that in the first vNav image, before any shim manipulation, the SVS voxel has a frequency offset of 0 Hz, as adjusted by the scanner. It should be noted that this failure has not been observed in other ROI's that are within the cerebrum and is exaggerated by the proximity of the cerebellum.

The second failure of the vNav PRESS sequence (n=4) was also specific to the cerebellum. It arises due to the presence of significant ghosting and distortions in the vNav volumes that

render the B0 field maps unusable to calculate a vNav-specific B0 shim. All four scans that failed in this manner had at least one second order shim term set greater than 1650 μT/m^2, which approaches the shim gradient limit. We believe that these large second-order shim gradients gave rise to EPI ghosts and distortions. From experience, increasing the volume over which the scanner adjusts these second order terms could provide more stable and less extreme values. In the future the B0 shimming algorithm used to calculate the higher order B0 shims should be reasonably constrained, or improved high order shim gradient amplifiers and waveform generators should be used for real time adjustment of these gradients.

The third failure of the vNav PRESS sequence (n=2) was the result of substantial water over-suppression, resulting in a water saturated spectrum. Over-suppression was identified because the residual water had a π phase shift from the water sample spectrum of the same voxel. The navigator estimated a shim magnitude of 350 μT/m; this is an offset from that set by the scanner. It is possible that the subject was in a different position or moving during the scanner's shim and water suppression optimisation process, leading to a substantially different optimal shim to that at the start of the SVS scan.

The navigator tracks a subject's movement and maintains a subject-specific coordinate system during the scan, defined by the reference TR. None of the children moved enough to cause a voxel shift greater than 3 mm during the scan. They did, however, exhibit small movements as shown in Figure 4. These were generally within a single TR, similar to what might be expected from swallowing or coughing.

The offline correction software presented here has been found to be simple and robust, requiring no user interaction. The advantage of cross-correlating a spectral range with a simulated spectrum is that it combines the contributions from several metabolites to find the frequency, thus making it robust to noise and variations in the residual water. The choice of SVD to calculate weights for weighted averaging enables the effective minimisation of spectra that do not fit the spectral trend, such as those perturbed by rapid movement. Further, as the SVD operation is performed on complex data, the weights generated are inherently complex, enabling phase-coherent averaging.

Conclusions

We have demonstrated marked improvement in the successful acquisition of MRS data in school-age children when acquisitions using the standard PRESS sequence are compared with those acquired using vNav PRESS. The vNav PRESS sequence, which improved spectral quality for all the children, enabled us to acquire usable data even from the most severely affected children with FAS. The vNav provides a consistent within scan VOI location while maintaining an optimal B0. We have demonstrated improved spectral quality when using the vNav in conjunction with offline preprocessing software as well as a reduced range and variance of metabolite concentrations. These benefits come at no extra time investment to the end user and no technical or additional equipment costs when scanning in standard brain regions.

Acknowledgments

This research was funded by grants from the South African Research Chairs Initiative of the Department of Science and Technology and National Research Foundation of South Africa, Medical Research Council of South Africa, NIH/National Institute on Alcohol Abuse and Alcoholism (R21AA017410, R01AA016781, R01 AA09524, U01 AA014790, and U24 AA014815) and the University of Cape Town, Wayne State University, and Joseph Young, Sr., Fund from the State of Michigan. We thank Siemens, Bruce Spottiswoode, Ph.D., the CUBIC radiographers Marie-Louise de Villiers and Nailah Maroof, Lindie du Plessis for assistance with LCModel analyses, Mathematician/Physicist M. Dylan Tisdall, our UCT and WSU research staff Maggie September, Nicolette Hamman, Mariska Pienaar, Emma Makin, and Neil Dodge. We also thank the dysmorphologists, H. Eugene Hoyme, Luther K. Robinson, and Nathanial Khaole, who conducted the dysmorphology diagnostic examinations of the children for FASD, funded by U01 and U24 grants from the Collaborative Initiative on Fetal Alcohol Spectrum Disorders (listed above). We also greatly appreciate the participation of the mothers and children in the longitudinal study.

References

Carter RC, Jacobson SW, Molteno CD, Chiodo LM, Viljoen D, Jacobson JL. Effects of prenatal alcohol exposure on infant visual acuity. J Pediatr. 2005; 147:473–479. [PubMed: 16227033]

Cheng DT, Meintjes EM, Stanton ME, Desmond JE, Pienaar M, Dodge NC, Power JM, Molteno CD, Disterhoft JF, Jacobson JL, Jacobson SW. Functional MRI of cerebellar activity during eyeblink classical conditioning in children and adults. Hum Brain Mapp. in press.

Coles CD, Platzman KA, Raskind-Hood CL, Brown RT, Falek A, Smith IE. A comparison of children affected by prenatal alcohol exposure and attention deficit, hyperactivity disorder. Alcohol Clin Exp Res. 1997; 21:150–161. [PubMed: 9046388]

Croxford J, Viljoen D. Alcohol consumption by pregnancy women in the Western Cape. South Afr Med J. 1999; 89:962–965.

Diwadkar VA, Meintjes EM, Goradia D, Dodge NC, Warton C, Molteno CD, Jacobson SW, Jacobson JL. Differences in cortico-striatal-cerebellar activation during working memory in syndromal and nonsymdromal children with prenatal alcohol exposure. Hum Brain Mapp. 2013; 34:1931–1945. [PubMed: 22451272]

Dimitrova A, Zeljko D, Schwarze F, Maschke M, Gerwig M, Frings M, Beck A, Aurich V, Forsting M, Timmann D. Probabilistic 3D MRI atlas of the human cerebellar dentate/interposed nuclei. Neuroimage. 2006; 30(1):12–25. [PubMed: 16257240]

Ernst T, Li J. Phase navigators for localized MR spectroscopy using water suppression cycling. Proc Int Soc Magn Res Med. 2009:239.

Gabr RE, Sathyanarayana S, Schär M, Weiss RG, Bottomley PA. On restoring motion-induced signal loss in single-voxel magnetic resonance spectra. Magn Res Med. 2006; 56:754–760.

Graverondemilly D, Diop A, Briguet A, Fenet B. Product-operator algebra for strongly coupled spin systems. J Magn Res Series A. 1993; 101:233–239.

Helms G, Piringer A. Restoration of motion-related signal loss and line-shape deterioration of proton MR spectra using the residual water as intrinsic reference. Magn Res Med. 2001; 46:395–400.

Henry PG, van de Moortele PF, Giacomini E, Nauerth A, Bloch G. Field-frequency locked in vivo proton MRS on a whole-body spectrometer. Magn Res Med. 1999; 42:636–642.

Hess AT, Tisdall MD, Andronesi OC, Meintjes EM, van der Kouwe AJW. Real-time motion and B0 corrected single voxel spectroscopy using volumetric navigators. Magn Res Med. 2011; 66:314–323.

Hess AT, Andronesi OC, Tisdall MD, Sorensen AG, van der Kouwe AJW, Meintjes EM. Real-time motion and B0 correction for localized adiabatic selective refocusing (LASER) MRSI using echo planar imaging volumetric navigators. NMR Biomed. 2012; 25:347–358. [PubMed: 21796711]

Hess AT, van der Kouwe AJW, Mbugua K, Laughton B, Meintjes EM. Quality of 186 child brain spectra using motion and B0 shim navigated single voxel spectroscopy. J Magn Res Imaging. in press.

Hollingshead, AB. Unpublished manuscript. Yale University; 1975. Four factor index of social status.

Hoyme HE, May PA, Kalberg WO, Kodituwakku P, Gossage JP, Trujillo PM, Buckley DG, Miller JH, Aragon AS, Khaole N, Viljoen DL, Jones KL, Robinson LK. A practical clinical approach to

diagnosis of fetal alcohol spectrum disorders: Clarification of the 1996 Institute of Medicine criteria. Pediatr. 2005; 115:39–47.

Jacobson JL, Jacobson SW, Molteno CD, Odenhaal H. A prospective examination of the incidence of heavy drinking during pregnancy among Cape Coloured South African women. Alcohol Clin Exp Res. 2006; 30:233A. [PubMed: 16441272]

Jacobson JL, Dodge ND, Burden MJ, Klorman R, Jacobson SW. Number processing in adolescents with prenatal alcohol exposure and ADHD: Differences in the neurobehavioral phenotype. Alcohol Clin Exp Res. 2011; 35:431–442. [PubMed: 21158874]

Jacobson SW, Jacobson JL, Sokol RJ, Chiodo LM, Corobana R. Maternal age, alcohol abuse history, and quality of parenting as moderators of the effects of prenatal alcohol exposure on 7.5 year intellectual function. Alcohol Clin Exp Res. 2004; 28:1732–1745. [PubMed: 15547461]

Jacobson SW, Stanton ME, Molteno CD, Burden MJ, Fuller DS, Hoyme HE, Robinson LK, Khaole N, Jacobson JL. Impaired eyeblink conditioning in children with fetal alcohol syndrome. Alcohol Clin Exp Res. 2008; 32:365–372. [PubMed: 18162064]

Jacobson SW, Stanton ME, Dodge NC, Pienaar M, Fuller DS, Molteno CD, Meintjes EM, Hoyme HE, Robinson LK, Khaole N, Jacobson JL. Impaired delay and trace eyeblink conditioning in school-age children with fetal alcohol syndrome. Alcohol Clin Exp Res. 2011; 35:250–64. [PubMed: 21073484]

Jenkinson M. Fast, automated, N-dimensional phase-unwrapping algorithm. Magn Res Med. 2003; 49:193–197.

Keating B, Deng W, Roddey JC, White N, Dale A, Stenger VA, Ernst T. Prospective motion correction for single-voxel 1H MR spectroscopy. Magn Res Med. 2010; 64:672–679.

Mattson SN, Riley EP, Gramling L, Delis DC, Jones KL. Heavy prenatal alcohol exposure with or without physical features of fetal alcohol syndrome leads to IQ deficits. J Pediatr. 1997; 131:718–721. [PubMed: 9403652]

Mattson SN, Crocker N, Nguyen TT. Fetal alcohol spectrum disorders: Neuropsychological and behavioral features. Neuropsychol Rev. 2011; 21:81–101. [PubMed: 21503685]

May PA, Booker L, Gossage JP, Croxford J, Adnams C, Jones KL, Robinson L, Viljoen D. Epidemiology of fetal alcohol syndrome in a South African community in the Western Cape Province. Am J Pub Health. 2000; 90:1905–1912. [PubMed: 11111264]

May PA, Gossage JP, Marais AS, Adnams C, Hoyme HE, Jones KL, Robinson LK, Khaole N, Snell C, Kalberg WO, Hendricks L, Brooke L, Stellavato C, Viljoen D. The epidemiology of fetal alcohol syndrome and partial FAS in a South African community. Drug Alcohol Depend. 2007; 88:259–271. [PubMed: 17127017]

May PA, Gossage JP. Maternal risk factors for fetal alcohol spectrum disorders: Not as simple as it might seem. Alc Research Health. 2011; 34:15–26.

Meintjes EM, Jacobson JL, Molteno CD, Gatenby JC, Warton C, Cannistraci CJ, Hoyme HE, Robinson LK, Khaole N, Gore JC, Jacobson SW. An fMRI study of number processing in children with fetal alcohol syndrome. Alcohol Clin Exp Res. 2010; 34:1450–1464. [PubMed: 20528824]

Molteno CD, Jacobson JL, Carter RC, Dodge NC, Jacobson SW. Infant emotional withdrawal: A precursor of affective and cognitive disturbance in fetal alcohol spectrum disorders. Alcohol Clin Exp Res. in press.

Provencher SW. Automatic quantitation of localized in vivo 1H spectra with LCModel. NMR Biomed. 2001; 14:260–264. [PubMed: 11410943]

Star-Lack JM, Adalsteinsson E, Gold GE, Ikeda DM, Spielman DM. Motion correction and lipid suppression for 1H magnetic resonance spectroscopy. Magn Res Med. 2000; 43:325–330.

Stratton, K.; Howe, C.; Battaglia, F. Fetal Alcohol Syndrome: Diagnosis, Epidemiology, Prevention, and Treatment. National Academy Press; Washington, DC: 1996.

Streissguth AP, Barr HM, Sampson PD. Moderate prenatal alcohol exposure: effects on IQ and learning problems at age 7.5 years. Alcohol Clin Exp Res. 1990; 14:662–669. [PubMed: 2264594]

Thesen S, Heid O, Mueller E, Schad LR. Prospective acquisition correction for head motion with image-based tracking for real-time fMRI. Magn Res Med. 2000; 44:457–465.

Thiel T, Czisch M, Elbel GK, Hennig J. Phase coherent averaging in magnetic resonance spectroscopy using interleaved navigator scans: Compensation of motion artifacts and magnetic field instabilities. Magn Res Med. 2002; 47:1077–1082.

Urban M, Chersich MF, Fourie LA, Chetty C, Olivier L, Viljoen D. Fetal alcohol syndrome among Grade 1 schoolchildren in Northern Cape Province: Prevalence and risk factors. South African Medical Journal. 2011; 98:877–882. [PubMed: 19177895]

Waddell KW, Avison MJ, Joers JM, Gore JC. A practical guide to robust detection of GABA in human brain by J-difference spectroscopy at 3 tesla using a standard volume coil. Magn Res Imaging. 2007; 25:1032.

Wechsler, D. WISC-IV Administration Manual. San Antonio, TX: The Psychological Corporation; 2003.

Zaitsev M, Speck O, Hennig J, Büchert M. Single-voxel MRS with prospective motion correction and retrospective frequency correction. NMR Biomed. 2010; 23:325–332. [PubMed: 20101605]

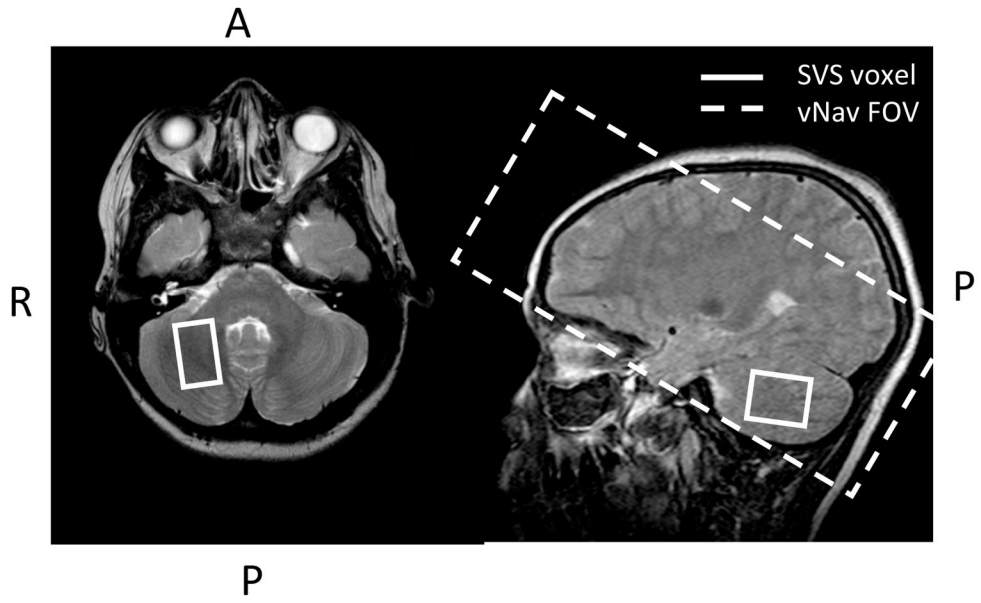

Fig. 1.

A) SVS volume of interest in the cerebellar deep nuclei, shown overlaid on the corresponding localising T2 turbo spin echo images B) Navigator FOV placement for scans with VOI in the cerebellum, it is angulated to ensure coverage of the cerebellum without increasing navigator duration

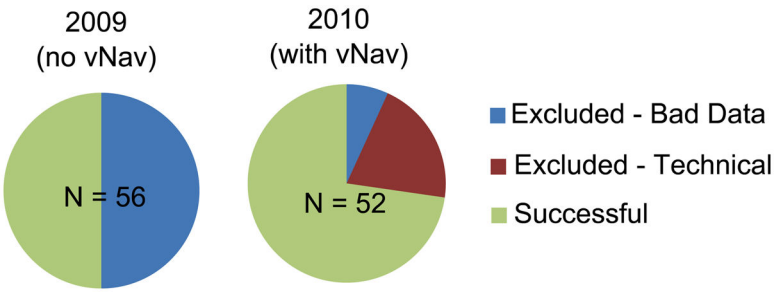

Fig. 2.

Pie charts showing the proportion of data excluded from each of the data sets due to either bad quality spectra or technical failures of the navigator

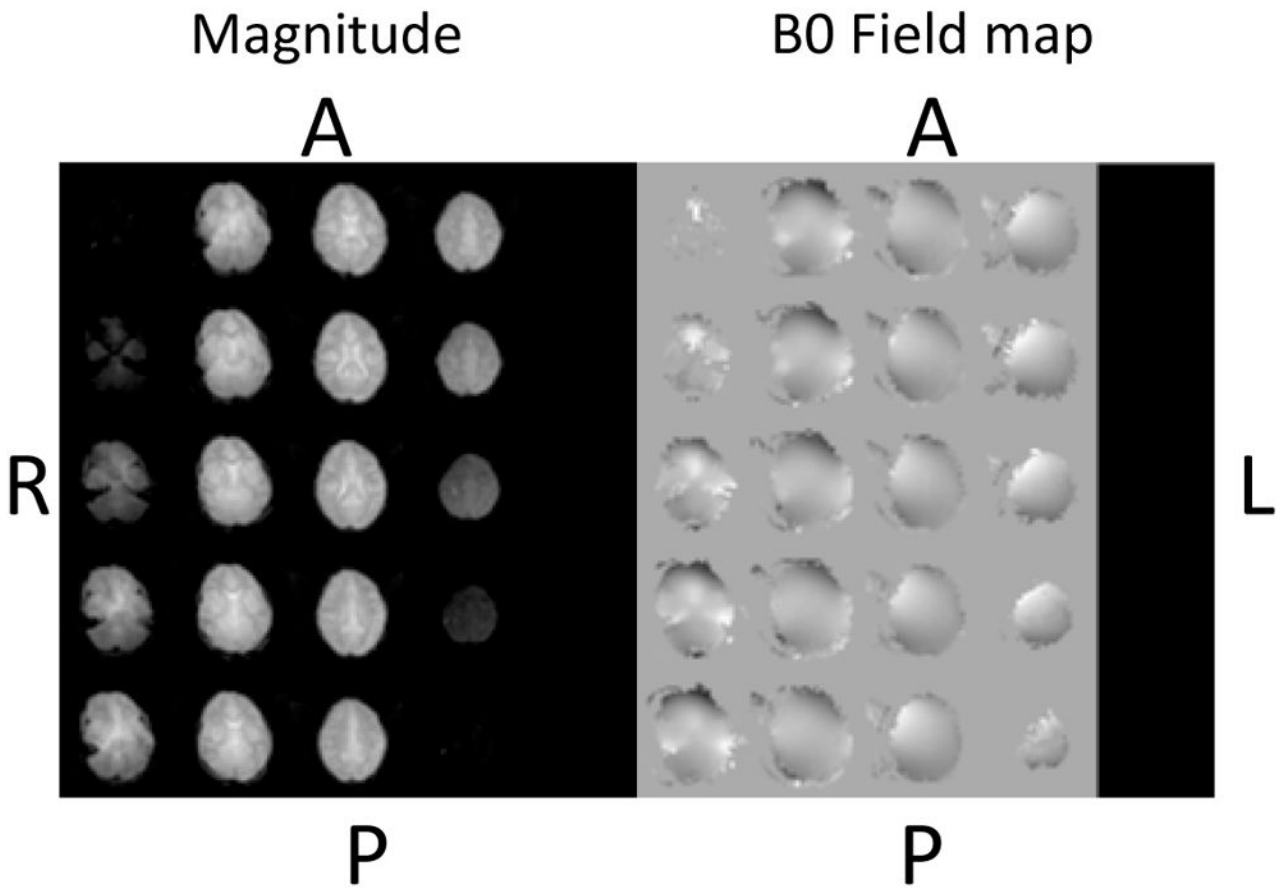

Fig. 3.

Navigator: magnitude image of first echo (used for PACE motion estimation) (left) and unwrapped field map (right)

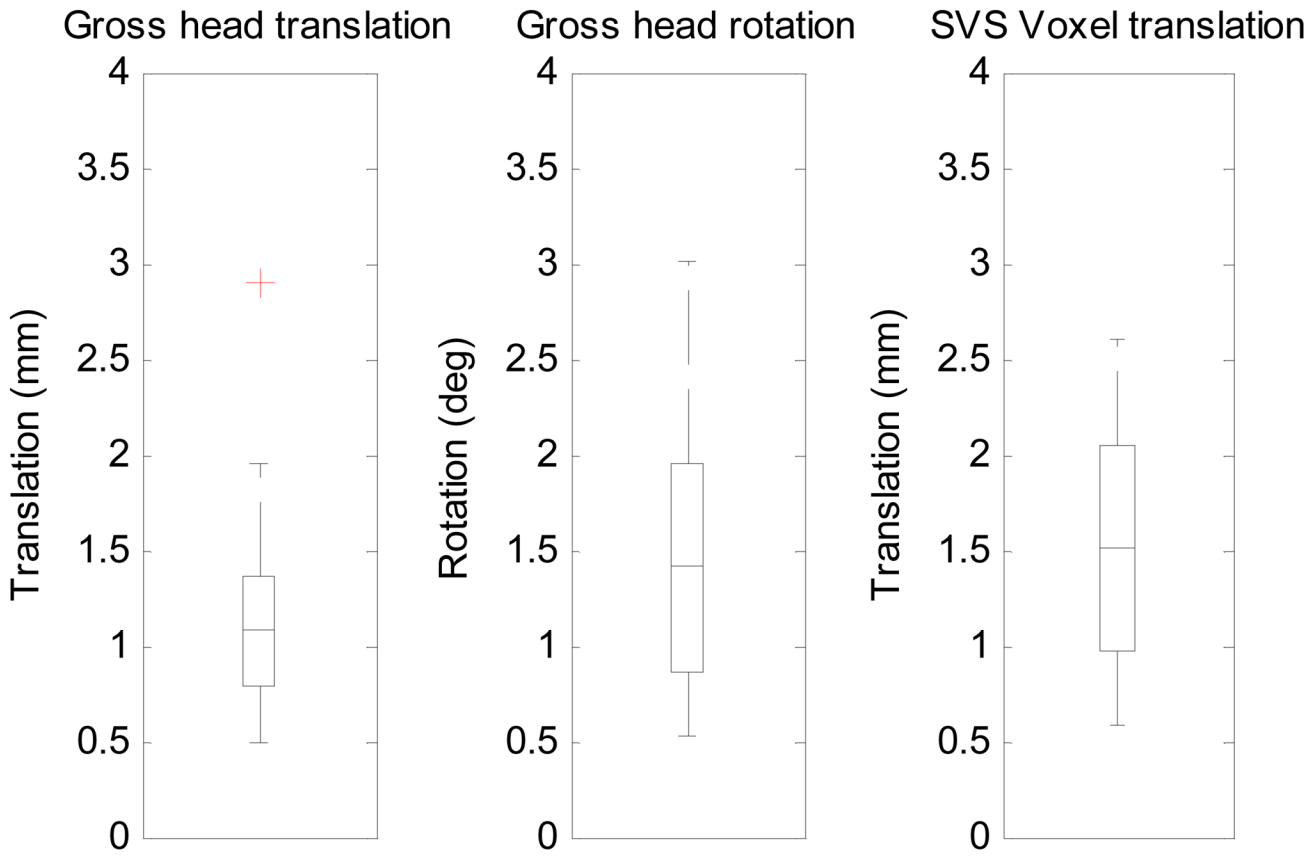

Fig. 4.

Box-and-whisker plots showing of the maximum absolute vector translations and rotations of the child's head from the start of the scan, expressed firstly about the centre of the navigator volume, representing gross head rotation and translation, and secondly about the centre of the SVS voxel, translations only.

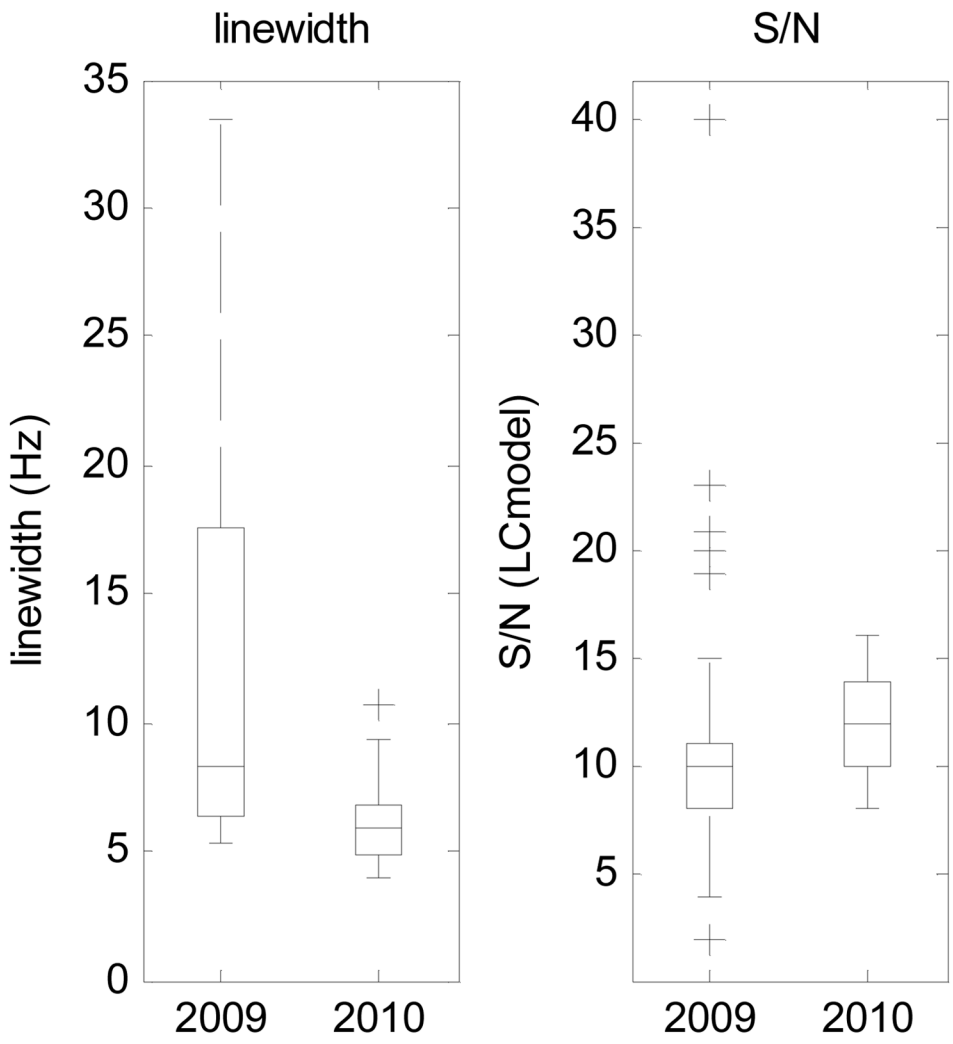

Fig. 5.

Box-and-whisker plots of linewidth and signal-to-noise ratio (S/N), as measured by LCModel, for all scans without the vNAV (2009) and all scans with the vNAV (2010)

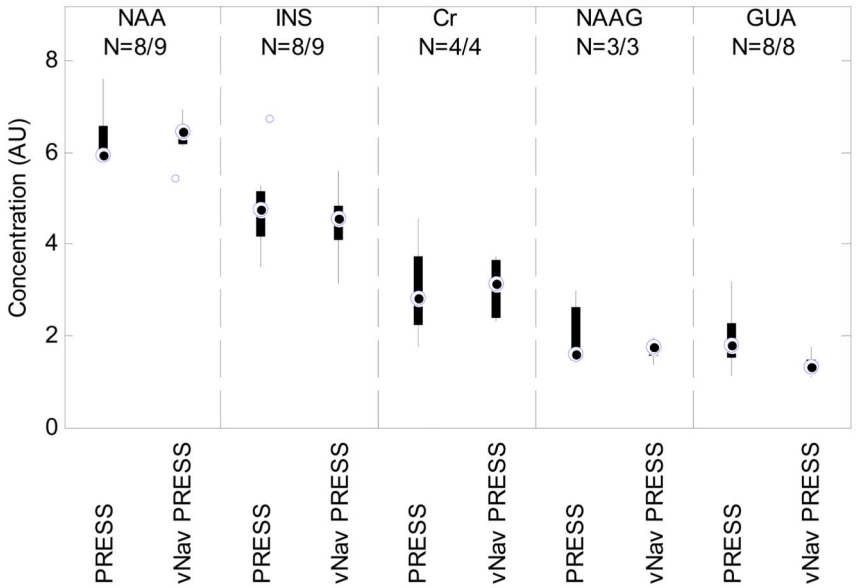

Fig. 6.

Box-and-whisker plots comparing the variance and range of metabolite concentrations in control children using the PRESS (2009) and vNav PRESS (2010) sequences. Data points were excluded if their %SD exceeded 30% with the resultant number of data points given by N.

Metab Brain Dis. Author manuscript; available in PMC 2015 June 01.

Table 1

Maternal and child background characteristics and prenatal exposure to alcohol, smoking, and marijuana by FASD diagnostic groups (N = 59)

	FAS (N = 9)	PFAS (N = 19)	Heavy exposed (N = 15)	Controls (N = 16)	F or χ^2
Maternal characteristics					
Education (years)	8.1 (1.7)	6.6 (2.3)	8.6 (2.9)	10.6 (1.6)	8.98***
Marital status (% married)	22.2	15.8	33.3	56.3	7.00†
Child characteristics					
Gender (% male)	33.3	57.9	53.3	50.0	1.54
Age at scan 1 (years)	9.3 (0.3)	9.4 (0.3)	9.6 (0.6)	9.4 (0.4)	1.61
Age at scan 2 (years)	10.0 (0.5)	10.5 (0.4)	10.5 (0.3)	10.3 (0.3)	2.93*
WISC-IV IQ[a]	64.4 (8.6)	64.1 (10.2)	73.1 (8.0)	76.4 (9.1)	6.96***
Prenatal exposure					
Cigarettes/day	7.7 (5.7)	7.7 (6.0)	8.1 (7.1)	2.2 (5.3)	3.39*
Alcohol[b]					
Absolute alcohol/day	1.8 (2.2)	1.0 (0.7)	0.5 (0.5)	0.001 (0.003)	7.55***
Absolute alcohol/occasion	4.8 (1.8)	3.6 (1.9)	2.7 (1.6)	0.1 (0.3)	23.60***
Frequency (days/week)	2.1 (1.8)	1.9 (1.1)	1.0 (0.9)	0.01 (0.02)	12.65***

Values are mean (SD) or %. 56 children were scanned in 2009 (9 FAS, 18 PFAS, 15 heavy exposed, 14 controls), and 55 in 2010 (7 FAS, 18 PFAS, 15 heavy exposed, 12 controls)

[a] Based on Wechsler Intelligence Scale for Children, 4th Edition.

[b] 1 oz absolute alcohol = the equivalent of about 2 standard drinks.

† $p < .10$

* $p < .05$

** $p < .01$

*** $p < .001$

Table 2

Technical failures of the vNAV by group for the 52 children scanned using the vNav PRESS acquisition in 2010.

Number of scans affected	Description	Total Exposed (FAS, *N* = 37)	Total Controls (*N* = 15)
5	Phase unwrapping algorithm generated a 2π phase offset, resulting in a frequency shift of 208 Hz. This rendered water suppression ineffective.	3	2
4	Ghosting in the first vNav EPI volume rendered the vNav unusable. This resulted from large shim terms set by the scanner for the voxel.	3	1
2	Water substantially over-suppressed (50% in these cases) as a result of a suboptimal pre-scan shim adjustment and resulting inappropriate water suppression adjustment.	2	0